International Journal of Engineering Research & Technology (IJERT)
NCAEM-2013 Conference Proceedings
ISBN: 978-93-83758-09-8

MICROWAVE DETECTION AND IDENTIFICATION OF BURIED METALLIC OBJECTS

[1]Praveen Sahwal, Assistant Professor(ECE),
Geeta Engineering College, Naultha,
(Panipat), Haryana, INDIA.

***Abstract*--In this paper the idea of using acoustically induced Doppler spectra as a means for metallic object detection and identification is introduced. Acousto-EM wave interaction occurs when an electromagnetic wave scatters from an object under acoustic illumination. The incident acoustic wave causes a boundary deformation within the metallic cylinder. The acoustically vibrating cylinder gives rise to a frequency modulated scattered electromagnetic field which is a function of the cylinder's natural resonance frequency and both the electromagnetic and acoustic source parameters. Results indicate that the scattered Doppler frequencies correspond to the mechanical vibration frequencies of the cylinder, and the sidelobe Doppler spectrum level is, to the first order, linearly proportional to the degree of deformation. The prior knowledge of doppler responses and signature of each metal help us to detect and identify the buried metallic cylinder.**

***Keywords*: - Electromagnetic Scattering, Acoustics, Metallic cylinders, Doppler spectrum, MATLAB.**

I. INTRODUCTION

Ground penetrating radars [3] have been used for detection and identification of buried objects. For civilian applications such radars are used to locate underground pipes, conduits, and cables, while military applications include mine detection and clearing abandoned military practice ranges of unexploded ordinance (UXO). If an identifiable Doppler spectrum is unique for the buried objects, corresponding to unique mechanical modes of the objects, then improvement in detection and identification of the objects is possible. In this approach,[4] object detection is based on the small changes in ground displacement when a buried object is introduced. The proposed scenario is shown in Fig. 1 In which an acoustic source launches an acoustic wave in the soil, mechanically exciting the buried objects, and electromagnetic radar measures the received electromagnetic spectrum from the vibrating objects. Significant displacement of an object only occurs when the object is excited at one of its acoustic resonances. Hence, the scattered electromagnetic Doppler spectrum will be composed of frequencies corresponding to the object's acoustic resonances. The frequency location of an object's resonances depends upon the object's shape and material properties and is generally different for different objects. In this technique, both acoustic and electromagnetic receivers are used to detect ground vibrations. As a feasibility study, we will examine, analytically, the Doppler scattering from a vibrating metallic circular cylinder in a homogeneous surrounding medium. Perturbation theory is an established analytical approach for scattering solutions and was applied by Rayleigh [5] and Maxwell [6] to certain scalar field problems. These methods have found application in electromagnetic scattering from rough surfaces [7, 8], cylinders [9, 10 and 11] and spheres [12, 13].

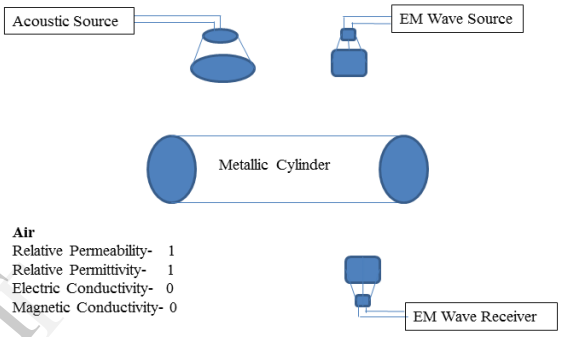

Fig. 1: Setup for object detection

I. ANALYTICAL DEVELOPMENT

Here, the bistatic scattered field from a perfectly conducting circular cylinder with arbitrary deformation and illuminated by an electromagnetic plane wave is formulated. An $e^{jw_e t}$ time dependence for electromagnetic waves and an $e^{jw_a t}$ time dependence for acoustic waves is understood in all expressions representing waves and is suppressed.

TM Mode

Consider an incident TM plane wave impinging upon a perfectly conducting, slightly deformed circular cylinder as shown in Fig. 2. For a vibrating cylinder whose cross section shape is varying with time, the scattered field will be time-varying which gives rise to the scattered Doppler spectrum. The perimeter of the cylinder's surface can be expressed in polar coordinates as

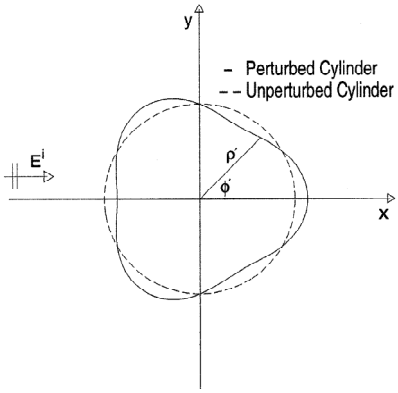

Fig. 2

ISBN: 978-93-83758-09-8

$$\rho' = a + bf(\emptyset', t) \quad -----(1)$$

Where a is the unperturbed cylinder radius, $f(\emptyset', t)$ is a periodic and smooth function of $\emptyset'$, and b is a perturbation constant assumed to be much smaller than the wavelength. The standard method for the computation of the scattered field from a circular cylinder is the eigen-function expansion of the total field. Following the development in [13], the incident plane wave propagating along the x-direction with a polarization parallel to the cylinder's axis can be expressed as

$$E_z^i = e^{-jk\rho cos\emptyset} = \sum_{n=-\infty}^{\infty} (-j)^n J_n(k\rho) e^{jn\emptyset} \quad ----(2)$$

Where k is the wavenumber. When there is no perturbation on the surface (i.e.,$b = 0$), the scattered field is given by

$$E_z^s = \sum_{n=-\infty}^{\infty} (-j)^n \frac{J_n(ka)}{H_n^{(2)}(ka)} H_n^{(2)}(k\rho) e^{jn\emptyset} \quad ----(3)$$

If a small perturbation is introduced on the boundary, the scattered field may be expanded in terms of a perturbation series in kb. To the first order in, we may write

$$E_z^s = \sum_{n=-\infty}^{\infty} (-j)^n \frac{J_n(ka)}{H_n^{(2)}(ka)} (1 + C_n kb) H_n^{(2)}(k\rho) e^{jn\emptyset} \quad --(4)$$

Where the C_n 's are unknown coefficients to be determined using the boundary condition $E_z^i + E_z^S = 0$ on the surface of the perturbed cylinder. This expression is, of course, a permissible solution of Maxwell's equations since it satisfies both the wave equation and the radiation condition. Using Taylor series expansion, the eigen-functions in (2) and (4) can also be approximated to the first order in kb, i.e.,

$$Z_n(k\rho') = Z_n\Big(k(a + bf(\emptyset', t))\Big) \approx Z_n(ka) + kbf(\emptyset', t) Z_n'(ka) \quad --(5)$$

Where Z_n represents the Bessel or Hankel function of nth order. Applying the boundary condition at the surface of the cylinder

$$\sum_{n=-\infty}^{\infty} (-j)^n [J_n(ka) + kbf(\emptyset', t) J_n'(ka)] e^{jn\emptyset'} = \sum_{n=-\infty}^{\infty} (-j)^n \frac{J_n(ka)}{H_n^{(2)}(ka)} (1 + C_n kb) \Big[H_n^{(2)}(ka) + kbf(\emptyset', t) H_n^{(2)'}(ka)\Big] e^{jn\emptyset'} \quad --(6)$$

Neglecting the $(kb)^2$ term and using the Wronskian relationship for Bessel functions results in the following expression:

$$\sum_{n=-\infty}^{\infty} (-j)^n C_n J_n(ka) e^{jn\emptyset'} = \frac{2jf(\emptyset', t)}{\pi ka} \sum_{n=-\infty}^{\infty} (-j)^n \frac{e^{jn\emptyset'}}{H_n^{(2)}(ka)} \quad ----(7)$$

Now if $f(\emptyset', t)$ has a Fourier series expansion with respect to $\emptyset'$

$$f(\emptyset', t) = \sum_{m=-\infty}^{\infty} A_m(t) e^{jm\emptyset'} \quad ----(8)$$

and is inserted into (7), the resulting solution for the coefficients, C_n, is

$$C_n(t) = \frac{2(j)^{n+1}}{\pi ka J_n(ka)} \sum_{p=-\infty}^{\infty} (-j)^p \frac{A_{n-p}(t)}{H_p^{(2)}(ka)} \quad ---(9)$$

Hence for a given displacement function, $f(\emptyset', t)$, the C_n 's calculated from (9) can be used in (4) to yield the bistatic scattered field at any angle . In this derivation it is implicitly assumed that the time rate of variations of $f(\emptyset', t)$ is much slower than the electromagnetic frequency so that relativistic effects can be neglected. Under this assumption, a Fourier transform of the time-varying scattered field will provide the scattered Doppler spectrum.

II. ACOUSTIC VIBRATION OF A SOLID CYLINDER

Mathematical Formulation for Displacement

In order to calculate the deformation of a circular cylinder due to a time-harmonic incident acoustic wave, the acoustic scattering from the cylinder must be evaluated. An interesting aspect of acoustic scattering from solid objects is that mechanical waves within the solid are excited which consist of both transverse shear waves and longitudinal compressional waves. The equation of motion for a solid elastic medium can be written [17]

The wave inside the cylinder will be represented by suitable solution of the equation of motion of a solid elastic medium, which may be written as

$$(\lambda + 2\mu)\nabla\Delta - \mu\nabla \times (2\omega) = \rho_1 \frac{\partial^2 u}{\partial t^2} \quad -----(10)$$

$$\frac{E(1-\sigma)}{(1+\sigma)(1-2\sigma)} \nabla(\nabla . u) - \frac{E}{2(1+\sigma)} \nabla \times (\nabla \times u) = \rho_1 \frac{\partial^2 u}{\partial t^2} \quad ----(11)$$

Where ρ_1 is the density of the scatterer, u is the displacement, and E and σ are Young's modulus and Poisson's ratio, respectively. Solutions to this equation for a solid cylinder of infinite length are of the form [16]

Where

$$\Delta = \nabla \cdot u \quad -----(12)$$

And

$$2\omega = \nabla \times u$$

From Eq. (14) can be derived the equations,

$$\nabla^2 \Delta = \Big(\frac{\rho_1}{\lambda} + 2\mu\Big) \frac{\partial^2 \Delta}{\partial t^2} \quad -----(13)$$

ISBN: 978-93-83758-09-8

And

$$\nabla^2(2\omega) = \left(\frac{\rho_1}{\mu}\right)\frac{\partial^2(2\omega)}{\partial t^2} \quad ----(14)$$

Which define the wave velocities

$$c_1 = \left[\frac{(\lambda+2\mu)}{\rho_1}\right]^{\frac{1}{2}} = \left[\frac{E(1-\sigma)}{\rho_1(1+\sigma)(1-2\sigma)}\right]^{\frac{1}{2}} \quad --(15)$$

And

$$c_2 = \left(\frac{\mu}{\rho_1}\right)^{\frac{1}{2}} = \left[\frac{E}{2\rho_1(1+\sigma)}\right]^{\frac{1}{2}} \quad ----(16)$$

Solution of Eq. (10) can be found by assuming that displacement can be derived from a scalar and a vector potential:

$$u = -\nabla\Psi + \nabla \times A. \quad ---- -(17)$$

The displacements thus can be thought of as the sum of two displacements, one associated with compressional waves and other with shear waves. If we assume that potentials satisfy the equations,

$$\nabla^2\Psi = \left(\frac{1}{c_1^2}\right)\frac{\partial^2\Psi}{\partial t^2} \quad ---- -(18)$$

And

$$\nabla^2 A = \left(\frac{1}{c_2^2}\right)\frac{\partial^2 A}{\partial t^2} \quad --(19)$$

the displacement derived from it shall be symmetrical about θ=0. Now, by Eq. (17) and (11),

$$u_r = \sum_{n=0}^{\infty}\left[\frac{nb_n}{r}J_n(k_2r) - a_n\frac{d}{dr}J_n(k_1r)\right]cosn\theta \quad --(20)$$

$$u_\theta = \sum_{n=0}^{\infty}\left[\frac{na_n}{r}J_n(k_1r) - b_n\frac{d}{dr}J_n(k_2r)\right]sinn\theta \quad --(21)$$

The factors c_n are the unknown coefficients which must be evaluated.

The following boundary conditions are applied at the surface of the cylinder:

$$p_i + p_s = -[rr] \quad at \quad r = a, \quad --(24)$$

$$u_{i,\,r} + u_{s,\,r} = u_r \quad at \quad r = a, \quad --(25)$$

And

$$[r\theta] = [rz] = 0 \quad at\ r = a. \quad ---(26)$$

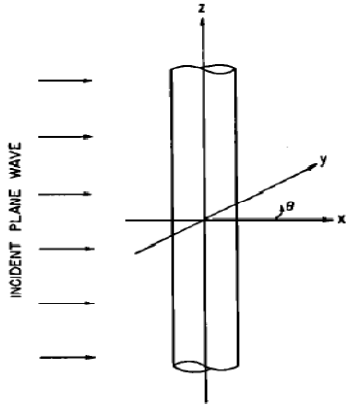

Fig. 3

By the conditions of symmetry, $[rz] = 0$ everywhere.Upon substitution from Eqs. (18), (19), (20), (22), (23), and (21), the boundary condition Eqs. (24), (25), and (26), for the nth mode solving these equations simultaneously for c_n. The result is

$$c_n = -P_0\varepsilon_n(-j)^{n+1}sin\eta_n \exp(j\eta_n), \quad --(27)$$

Mapping to Radial Displacement

The displacement of the cylinder is now represented by both a radial and angular displacement in (32) and (33). Recall that the perimeter of the cylinder is expressed from (1) as $\rho' = a + bf(\emptyset', t)$ with the radial displacement given by $bf(\emptyset', t)$. The radial and angular displacement can be mapped into only radial displacement by setting

$$bf(\emptyset', t) = u_r(\emptyset' - \emptyset_0, t) \quad -----(28)$$

Where $\emptyset_0$ is the angular shift corresponding to the angular component of displacement, $u_\emptyset$. Frombasic geometry (see Fig. 4) and an application of Taylor series about $\emptyset_0$

$$\emptyset_0 = \frac{u_\emptyset(\emptyset' - \emptyset_0, t)}{a} \approx \frac{u_\emptyset(\emptyset', t)}{a} - \emptyset_0\frac{u'_\emptyset(\emptyset', t)}{a} \quad --(29)$$

Solving for $\emptyset_0$

$$\emptyset_0 = \frac{u_\emptyset(\emptyset', t)}{a + u'_\emptyset(\emptyset', t)} \approx \frac{u_\emptyset(\emptyset', t)}{a} \quad --(30)$$

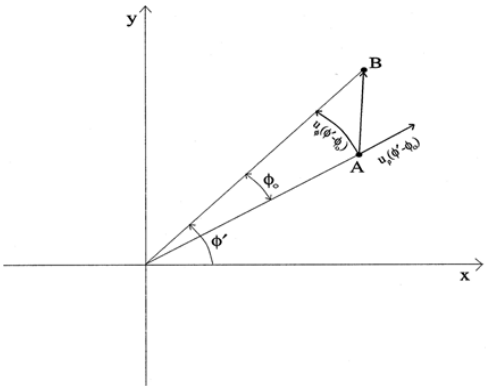

Fig. 4: Mapping Radial Displacement

Since $u'_\emptyset(\emptyset', t) \ll a$. And substituting (30) into (28) gives

$$bf(\emptyset', t) = u_r\left(\emptyset' - \frac{u_\emptyset(\emptyset', t)}{a}, t\right). \quad --(31)$$

Rewriting u_r and $u_\emptyset$ with time dependence explicitly shown

$$u_r(\emptyset', t) = \sum_{n=0}^{\infty} U_{r,n}\cos(w_a t + \theta_{\rho,n})\cos(n\emptyset') \quad --(32)$$

$$u_\emptyset(\emptyset', t) = \sum_{n=0}^{\infty} U_{\emptyset,n}\cos(w_a t + \theta_{\emptyset,n})\sin(n\emptyset') \quad --(33)$$

ISBN: 978-93-83758-09-8

Where $U_{r,n}$and $U_{\emptyset,n}$are the magnitudes of the coefficients for the n[th] mode given by the expressions in brackets in (20) and (21), respectively, and $\theta_{\rho,n}$and $\theta_{\emptyset,n}$are the respective phases of these coefficients. Substituting (32)and (33) into (31).

When only one mode has significant displacement, however, for the n[th] mode simplifies to

$$bf = U_{r,n}\mathrm{COS}(w_a t + \theta_{\rho,n})\, COS\left[n\left(\emptyset' - \frac{U_{\emptyset,n} COS(w_a t + \theta_{\emptyset,n})}{a} Sin(n\emptyset')\right)\right] \quad -- (34)$$

this expression should be expanded in a Fourier series about . The coefficients, $A_m(t)$, of the expansion can then be used in the TM or TE electromagnetic solution to obtain the time-varying scattered field. Taking $b = U_{r,n}$, we can expand $f(\emptyset', t)$in a Fourier series about $\emptyset'$.

III. SIMULATIONS

Doppler Response

Fig. 6 shows the calculated Doppler spectrum of the backscattered field with TM incidence for n=2 mode. The spectrum is similar to a frequency modulated signal with a low index of modulation. The spectrum has frequency components at harmonics of the incident acoustic frequency of which the first is by far the largest. Other acoustic modes produce a similar Doppler spectrum where the frequency components are at harmonics of the vibration frequency and the first component is still the most significant. When the frequency of the incident acoustic wave is not close to a resonant frequency of the cylinder, it behaves as a rigid cylinder. Consequently, there is negligible displacement at the surface of the cylinder, and the magnitude of the Doppler spectrum is also negligible. However, when the frequency of the incident acoustic wave is close to a resonance of the object, the mode corresponding to this resonance is excited and a measurable Doppler spectrum results.

Excitation at Resonance

Here, the magnitude of the first harmonic of the Doppler spectrum in the backscatter field is calculated as a function of the incident acoustic frequency. This illustrate the effect of resonance on the scattered Doppler spectrum. Fig. 7 show measured and computed first harmonic of the scattered Doppler spectrum for the cylinders of various material in air.

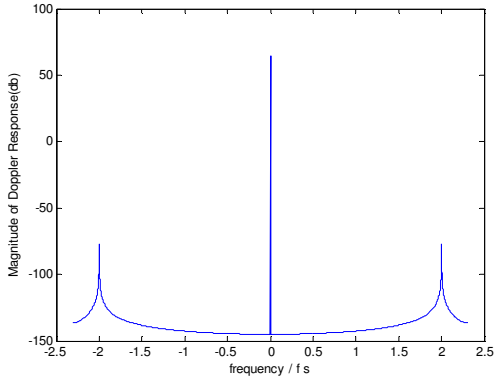

Fig. 6: Fourier transform of backscattered Doppler spectrum

The doppler response of the scattered field is plotted against acoustic frequency. This is highly sensitive to resonances in the cylinder. Note that the n=2 mode is resonant at the lowest frequency, followed by the n=1 andn=3 modes. Hence, by acoustically vibrating the cylinder over a wide range of frequencies, the Doppler response will have significant Doppler components only at the mechanical resonant frequencies of the cylinder.

Fig. 7 show the scattered doppler spectrum for Steel cylinder of radius 5cm for mode n=1 and 2. The young modulus is 200×10^9 Pascal, possoinratio is 0.28, density is 7.7 g/cm^3.

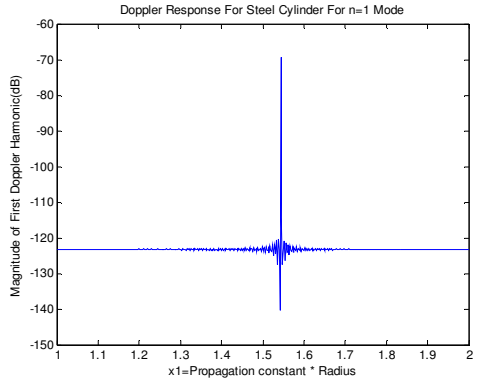

Fig. 7 (a): Doppler Response For Steel Cylinder For n=1 Mode

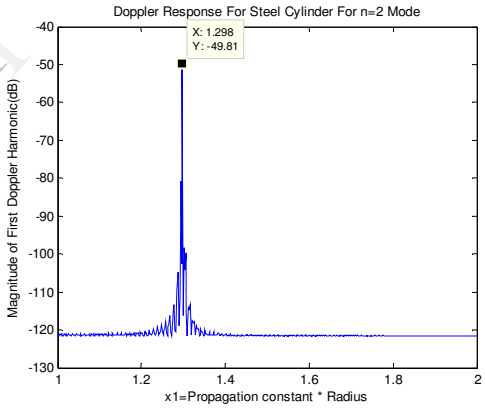

Fig. 7 (b): Doppler Response For Steel Cylinder For n=2 Mode

Here ,the profile of three cylinders of Aluminium, Steel and Brass is presented. If we have some knowledge of their pattren of doppler response and magnitude in advance, then we can easily detect the buried cylinders.

Three different mode of excitation of cylinder of different materials is given in the Table 1. In each mode cylinder has different resonant frequency and magnitude of doppler response. Resonant frequency, magnitude of doppler response and difference between 1[st] and 2[nd] harmonic of doppler response are the factors that differentiate the cylinder of different material. All these properties of different material are shown in Table 1.

This undesirable result is offset by realizing that in a practical scenario the buried objects of interest are likely to be metallic or plastic shells which will have significantly larger displacements (and lower resonant frequencies) than the virtually rigid, solid objects considered here.

ISBN: 978-93-83758-09-8

Doppler Response for Aluminium Cylinder				
Mode No.	X1=Propagation Constant *Radius	Resonant Frequency (KHz)	Magnitude of Doppler Response(dB)	Difference Between 1st and 2nd Harmonic
n=1	1.43	2.82	58	5dB
n=2	1.174	2.32	71	0.5dB
n=3	1.83	3.61	36	3dB

Table 1: Doppler Response for Aluminium Cylinder

IV. CONLUSION

In this work, the analytical Doppler spectrum of an acoustically vibrated circular cylinder is examined and which is strongly dependent upon the cylinder's mechanical resonances. An analytical solution for the bistatic scattering from a deformed cylinder is derived using a perturbation method. The Doppler spectrum consist of harmonics of the incident acoustic frequency where the first harmonic is the most significant. Also, the first harmonic only becomes measurable when the cylinder is excited near a mechanical resonance. These results indicatethat acoustically vibrating an object at its resonant frequencies and measuring the Doppler scattered response monostatically or bistatically could provide an effective method for detecting and identifying buried objects of different metals. Afer analysing the signature of different metals, it is concluded that the signature of metal buried under the ground have very sharp response, than as it happens in case of steel that can be property of an alloy. From the signature reflected from the different metals buried under the ground, it obsereved that the profile of that metal including amplitude doppler response for resonant frequency and its harmonic are found different for different metal where it is concluded using the profile of the reflected signature, we can identify the metal of the buried objects.

REFERENCES

[1]. Daniel E. Lawrence and Kamal Sarabandi, "Acoustic and Electromagnetic Wave Interaction: Analytical Formulation for Acousto-Electromagnetic Scattering Behavior of a Dielectric Cylinder", IEEE Trans. Antennas Propagation, VOL. 49, NO. 10, OCTOBER 2001

[2]. C. Stewart, "Summary of mine detection research," U.S. Army engineering res. and devel. labs, Corps. ofEng., Belvoir, VA, Tech. Rep.1636-TR, vol. I, pp. 172–179, May 1960.

[3]. G. S. Smith, "Summary report: Workshop on new directions for electromagnetic detection of nonmetallic mines," Report for U.S. Army BRDEC and ARO, June 1992.

[4]. W. R. Scott, Jr. and J. S. Martin, "An experimental model of a acousto-electromagnetic sensor for detecting land mines," in IEEE AP-S Int. Symp. Dig., Atlanta, GA, July 1998, pp. 978–981.

[5]. , "Experimental investigation of the acousto-electromagnetic sensor for locating land mines," Proc. of SPIE—Int. Society Optical Engineering, vol. 3710, no. I, pp. 204–214, 1999.

[6]. Daniel E. Lawrence and Kamal Sarabandi, "Electromagnetic Scattering from a Dielectric Cylinder Buried Beneath a Slightly Rough Surface", IEEE Trans. Antennas Propagat.

[7]. S. O. Ogunade, "Electromagnetic response of an embedded cylinder for line current excitation," Geophys., vol. 46, no. 1, pp. 45–52, Jan. 1981.

[8]. R. F. Harrington, Time-Harmonic Electromagnetic Fields. New York: McGraw-Hill, 1961, pp. 232–235.

[9]. J. J. Faran, "Sound scattering by solid cylinders and spheres," J. Acous. Soc. Amer., vol. 23, no. 4, pp. 405–418, July 1951.